Intensity Coding in the Frog Retina

Quantitative relations between impulse and graded activity

DWIGHT A. BURKHARDT and PAUL WHITTLE

From the Vision Laboratory, Department of Psychology, University of Minnesota, Minneapolis, Minnesota 55455

ABSTRACT The impulse discharge of single on-off neurons and a graded field potential, the proximal negative response (PNR), were simultaneously recorded with an extracellular microelectrode in the inner frog retina. Normalized amplitude-intensity functions for the on-response of the PNR and the neuron's poststimulus time histogram (PSTH) were nearly coincident and typically showed a dynamic range spanning approximately 2 log units of intensity. Thus a nearly linear relation is found between the amplitude of the PNR and the neuron's PSTH. A neuron's PSTH amplitude and maximum instantaneous frequency of discharge were usually highly correlated, but occasional marked disparities indicate that temporal jitter of the first spike latency is an additional, relatively independent variable influencing PSTH amplitude. It typically changes by a factor of 20–30 over the intensity range. These and other findings have implications for the functional significance of the PNR and the PSTH, for a possible linear link between amacrine and on-off ganglion cells, and for a mechanism of intensity coding in which temporal jitter of latency exerts a major role.

INTRODUCTION

The retinal code for the intensity of a visual stimulus is initiated by the absorption of light quanta in receptor photopigments, then expressed as graded variations in the slow potentials of distal cells, and ultimately transmitted to the brain as a pattern of all-or-none impulses in the optic nerve. This outline of the intensity coding process of the retina seems firmly established from classic work on visual pigments and ganglion cells and from recent intracellular recordings in several vertebrates (for review, Dowling and Werblin, 1971). But little is yet known about quantitative relations between graded and impulse activity in vertebrate retinas and even the quantitative features of the impulse intensity code of ganglion cells seem surprisingly unsettled (Brindley, 1970). In this paper, we attempt to deal with aspects of these issues.

With a metal microelectrode placed in the inner retina of the frog, we simultaneously record the impulse discharge of single on-off neurons along with the proximal negative response (PNR)—a graded field potential believed to monitor the activity of amacrine cells (Burkhardt, 1970). The special features of simultaneity and relative stability of these extracellular recordings permit rather detailed quantitative study of the effects of stimulus intensity on both responses. Our findings reveal an approximately linear relation between the amplitude of the PNR and the amplitude of the neuron's poststimulus time histogram (PSTH), lead us to consider the basis and functional significance of the PSTH, and to advance a simple mechanism for visual intensity coding in which temporal variability of the afferent discharge plays a major role.

MATERIALS AND METHODS

Preparation and Recording

Since most features of the preparation and recording are treated in detail elsewhere (Burkhardt, 1970), only particularly pertinent details are described here. Insulated platinum-iridium microelectrodes (tip $\leq$ 1 μm) were used to record light-evoked electrical activity from the leopard frog (*Rana pipiens*) eyecup, with the latter placed in a small chamber through which moist gas (95 % O_2–5 % CO_2) circulated. Potentials were led to a cathode follower and then to an AC amplifier (3 dB cutoffs at 0.2 and 1000 Hz) whose output was monitored on an oscilloscope and fed to an FM converter (0–1000 Hz bandwidth). The output of the converter was recorded on one channel of a stereo tape recorder and stimulus signals were recorded on the other.

In all experiments in this paper, we have operationally adjusted the electrode depth depth to that region at which the PNR is maximum. Previous work indicates that this corresponds to a region about 75 μm from the internal limiting membrane (Burkhardt, 1970; Fatechand, 1971; Tomita and Torihama, 1956), i.e. approximately at the border between the inner nuclear and inner plexiform layers. With the electrode so advanced, we could often record a well isolated on-off impulse discharge which was first clearly seen when the electrode lay more proximally, near or upon the retinal surface. Such on-off units have commonly been assumed to be ganglion cells, but there is now evidence from intracellular work in fish, mudpuppy, and frog that some amacrine cells also generate on-off spike discharges (Kaneko, 1970; Werblin and Dowling, 1969; Matsumoto and Naka, 1972). Since there are as yet no certain criteria to decide if an extracellularly recorded on-off discharge arises from a ganglion cell or an amacrine cell, we will use the general term, neuron, when describing our single unit results. However, in part of the discussion we depart from this policy and use some main features of our results to suggest several hypotheses about on-off ganglion cells. We think this is warranted since the response properties of our units seem very similar to those described for frog on-off optic nerve fibers (Hartline, 1938, 1940 *a*, 1940 *b*; Maturana et al., 1960; Grüsser-Cornehls et al., 1963) and to those recorded with large electrodes from the surface of the frog retina (Granit, 1963; Barlow, 1953 *a*, 1953 *b*). The spikes of all the units considered below were biphasic and initially negative in

polarity. Here we deal only with the on-response, but all units also gave a vigorous off-discharge when tested with 1 s flashes. Some properties of the on-response of these neurons are summarized in Table I.

Stimulation and Procedures

Responses were evoked by flashing a 100 μm diameter spot of white light for 200 ms once every 10 s upon a uniform background field (0.1 foot-candle) which covered the entire retina. The optical system has been described (Burkhardt and Berntson, 1972). Since we could typically hold a stable unit recording no longer than 1–1½ h, the conditions used represent an attempt to obtain an adequate sample of data within the time available. For this reason, we chose to record 16 responses at about seven intensity levels. A relatively short flash (200 ms) and a moderately long interstimulus interval (10 s) were used to minimize interaction between successive flashes and intensity levels. Although auxilliary experiments suggest that the responses obtained for maximum intensities are subject to some diminution (about 15% below that which would be obtained with a single well spaced flash of the same intensity), the PNR amplitude-intensity curves which we show below (Fig. 4) are generally quite similar in form and range to those found in earlier work using single flashes spaced every 20 s (Burkhardt, 1970). We therefore doubt that the 10 s interstimulus interval seriously affects any major conclusions about intensity coding which we advance below.

The essential steps of the procedure were: (*a*) After adjusting electrode depth (see above) and stimulus position to obtain a maximum PNR, stimulation was stopped for about 5 min. (*b*) Dim flashes were then presented and their intensity increased until a minimum stimulus level was found which consistently evoked an impulse discharge. (*c*) 20 flashes at that intensity were presented and the last 16 responses were recorded. (*d*) Step *c* was repeated at successively higher intensities until the PNR amplitude and maximum frequency of the impulse discharge gave evidence of saturation. Following this routine, we typically obtained response samples at seven intensity levels.

After completing these steps, stimulation was stopped for about 5 min. The receptive field of the neuron was then mapped in the standard way: At each of a series of stimulus positions, the 100 μm test spot was flashed four times at each of a series of intensity levels which spanned the threshold region. The number of times an impulse discharge occurred at each intensity was recorded and this measure used to determine the intensity for which the probability of response was 0.5, interpolating in those cases where no intensity used gave precisely two responses for four presentations. The reciprocals of the threshold intensities were then plotted against stimulus position to yield the neuron's receptive field profile.

About 30 retinas were used in the course of this work. Many on-off units were initially well isolated and 11 of these were held long enough to complete the basic intensity series described above. Of these, three were lost before the receptive field map was finished.

Data Analysis

After an experiment, responses were played back from tape and several analyses performed with a Fabri-Tek 1064 computer (Nicolet Instrument Corp., Madison, Wis.).

The raw responses consisted of nerve impulse activity superimposed upon the PNR (see Fig. 1). With the computer's low pass filter appropriately set, impulse activity could be eliminated without distorting the PNR and average PNR's for sets of 16 identical stimuli were obtained and written out with an $x - y$ plotter.

To analyze spike activity, a high pass filter was used to remove the PNR and the impulses were fed to a discriminator network which sent a standard pulse to the computer for each impulse. The computer was set in the count mode and the neuron's poststimulus time histogram (PSTH) was thus extracted for sets of 16 stimuli. To insure that no spurious counts occurred, the impulse discharge and the pulse input to the computer were simultaneously monitored on an oscilloscope. In early work, bin widths from 2 to 10 ms were used. Apart from more ragged waveforms for the small bin widths, no marked width-dependent effects were noted. We thus settled on an intermediate bin width of 6 ms and have used it in all the PSTH measurements discussed below.

As this work proceeded, it seemed of interest to evaluate the maximum instantaneous frequency and the first spike latency of each impulse discharge, neither of which can be unequivocally derived from the PSTH. We therefore used the computer in the count mode and displayed individual responses with the $x - y$ plotter. By appropriate setting of sweep speed and size of the plotter display, these records could be read to an accuracy of about ∓ 0.2 ms. Below we emphasize the possible functional significance of temporal variability of the impulse discharge, so we may note here that repeated playbacks of the same response were reproducible to a few 10ths of a millisecond, and even more to the point, the variability which concerns us below is a function of stimulus intensity and thus clearly the property of the response and not the recording system.

RESULTS

Fig. 1 introduces most of the general observations which we will analyze in some detail in the remainder of this report. The microelectrode has been advanced to an optimum depth in the inner retina (see Methods). A small spot of light is now flashed for 200 ms at several intensity levels as indicated by the logarithmic units to the left. For all but the lowest intensity, the on-discharge of a single on-off neuron can be seen as a burst of spikes superimposed upon a negative graded potential, the proximal negative response (PNR). Similar recordings have been recently observed in the pigeon retina (Holden, 1972). To use them for quantitative study, we must first consider the spatial properties of each response in relation to the stimulation used.

The amplitude of the PNR is very critically dependent on stimulus position (Burkhardt, 1970; Burkhardt and Berntson, 1972). Therefore, in Fig. 1 and throughout the present study, we always place the stimulus at the operationally determined position at which the evoked PNR is maximum. It is thus quite important to know how this position relates to the receptive field dimensions of the on-off neurons whose activity we simultaneously record. Receptive field maps are shown in Fig. 2 for five neurons, including neuron C whose responses appear in Fig. 1. They are in good general agreement with

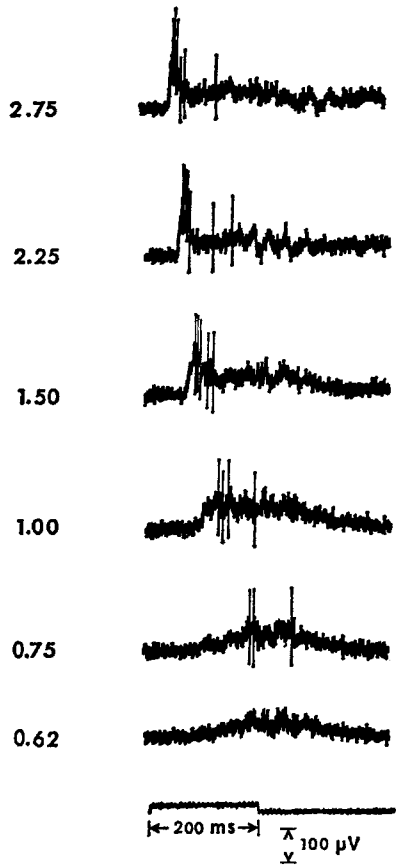

FIGURE 1. Simultaneous recordings of the PNR and the impulse discharge of an on-off neuron. Responses evoked by flashing a 100 μm diameter spot at a series of intensity levels indicated in logarithmic units at left (0.75 = 0.03 foot-candle). Lowest trace is a photocell record of the stimulus. Background illumination: 0.1 foot-candle.

previous findings in the frog (Barlow, 1953 *b*; Hartline, 1940 *a*, Reuter, 1969). Now the arrows in Fig. 2 show the position at which the PNR is maximum when using the same spot size (100 μm) as that used to map the receptive field, and show that the optimum position for the PNR lies very near or within the central region of the neuron's receptive field. The stimulus positions used in the present work are therefore appropriate for efficiently activating both PNR and neuron and hence, for studying the quantitative relations between the two types of response. The stimulus diameter (100 μm) is similarly appropriate for, as recently shown (Burkhardt and Berntson, 1972), a spot of 100 μm falls within the central summation zone of the two response mechanisms and covers about half of the spatial channels which efficiently convey excitation to them.

Having clarified the spatial conditions under which our observations are

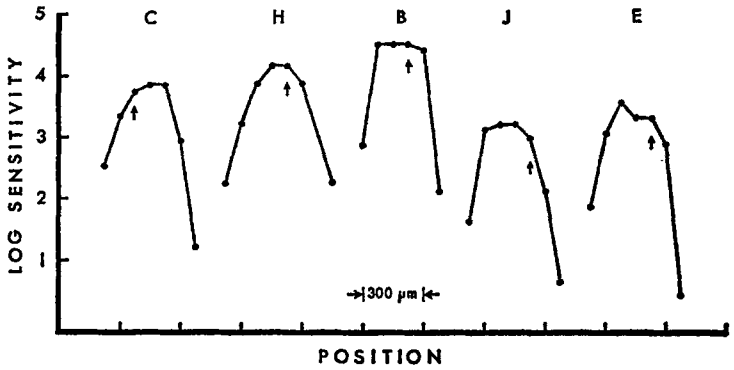

FIGURE 2. Receptive field profiles of on-off neurons from five different retinas. Arrow indicates the stimulus position at which the PNR is recorded at maximum amplitude. Log sensitivity of 3.0 is equivalent to a stimulus of 0.1 foot-candle. Background illumination: 0.1 foot-candle.

made, we now return to Fig. 1 and summarize some general findings illustrated there: (*a*) The bottom trace shows that a weak stimulus which fails to evoke an impulse discharge still evokes a small but clearly detectable PNR. This was noted earlier (Burkhardt, 1970), was invariably observed in the present work, and should be born in mind later when comparing the lowest portions of the amplitude-intensity curves for PNR and neurons. (*b*) The first spike of the neural discharge occurs after the onset of the PNR. This was always observed for individual responses and merits emphasis here since this feature of the relation between PNR and impulse activity is somewhat obscured in the average response measures used below. (*c*) The marked tendency for the first spike to occur at higher PNR voltage levels as intensity increases is seen in Fig. 1, was generally observed, and also held clearly when comparisons were made between median first spike latency and the computer-averaged PNR waveform. Thus, the first spike of the discharge is not triggered when the PNR reaches a constant level. (*d*) The vigor of the neural discharge and the amplitude of the PNR seem to increase over a similar range of intensity. To pursue this quantitatively, we first examine the relation between the PNR and the neuron's poststimulus time histogram (PSTH).

Fig. 3 shows the average PNR's and the PSTH's obtained for the same neuron and flash intensities as of Fig. 1. These responses are based on 16 stimulus repetitions per intensity level (see Methods). The PSTH's emphasize the highly phasic nature of the neuron's response and this is typical of all neurons considered in this paper. Particularly at the higher intensities (Fig. 3), most of the spikes in the PSTH cluster around a rather sharp peak and the discharge is effectively over within about 100 ms. And so even with the capacitatively-coupled amplification, metal microelectrodes and short flash duration used here, the PNR may be seen to clearly outlast the dura-

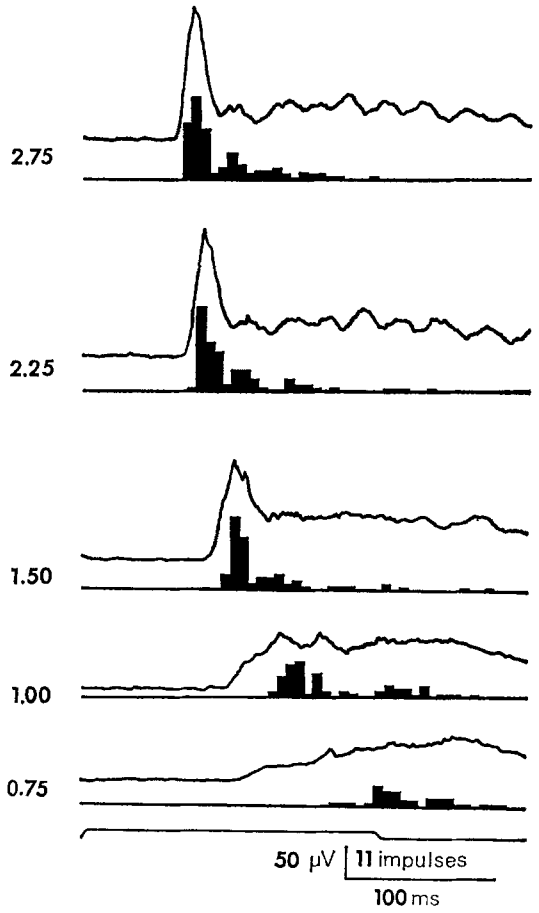

FIGURE 3. PSTH of an on-off neuron and the average PNR evoked by flashes of different intensities as indicated to the left. Same neuron, stimulus conditions, and intensity notation as in Fig. 1. Responses are based on 16 stimulus repetitions per intensity level.

tion of the spike discharge. Thus, although there is a tendency for the late spikes to be associated with the small late oscillations in the PNR (and this is often clearly seen in individual responses), these retinal recordings may be contrasted with those in cat visual cortex where the waveforms of the PSTH of a single neuron and the simultaneously recorded field potential are often nearly identical (Fox and O'Brien, 1965).

In Fig. 3 there is a marked similarity in the way the peak amplitudes of the PNR and PSTH vary with intensity and we have found this to hold for all neurons studied. Fig. 4 shows amplitude-intensity curves for the five neurons whose receptive fields were shown in Fig. 2. The closed circles represent the peak amplitude of the neuron's PSTH while the open circles indicate the peak amplitude of the PNR. Both measures are normalized relative to the

maximum response obtained in each preparation. (see the p_{max} and a_{max} columns in Table I for absolute values of the maximum responses.) The results in Fig. 4 have been selected from our total sample of 11 to include cases giving broad (*E*) and narrow (*C*) dynamic ranges. The PNR dynamic

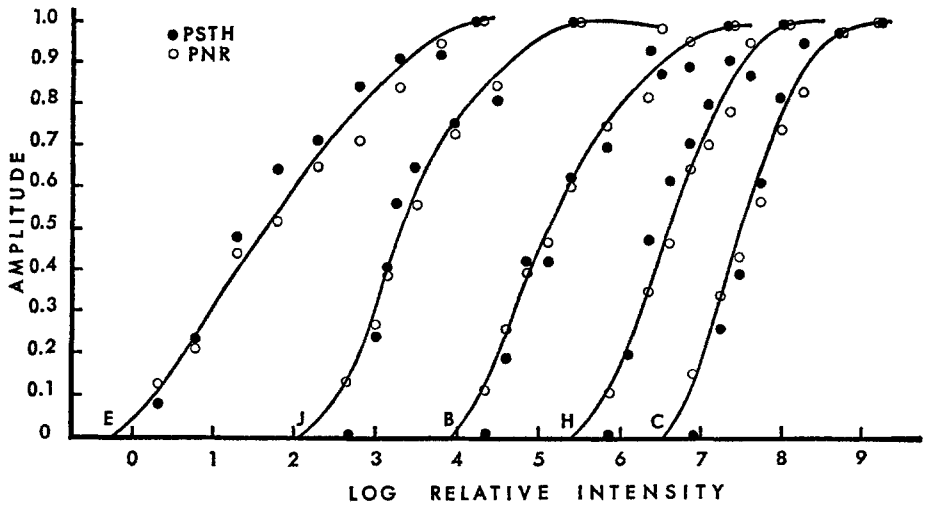

FIGURE 4. Amplitude-intensity curves for the PSTH of five on-off neurons (filled circles) and for the simultaneously recorded PNR (open circles). The smooth curves are drawn by eye and their relative lateral separations are arbitrary. See Fig. 2 for absolute sensitivity of the neurons.

TABLE I

SUMMARY OF ON-RESPONSE PARAMETERS

Preparation	p_{max}	f_{max}	n_{max}	$Q_{L_{max}}$	$Q_{L_{min}}$	a_{max}	D
A	31	348	4.7	25	4.0	260	1.65
B	26	295	8.9	24	1.0	150	2.10
C	29	284	6.9	16	1.0	175	1.80
D	21	216	6.2	49	1.0	260	2.60
E	26	286	6.1	27	1.6	300	3.05
F	25	253	5.3	56	1.6	650	3.25
G	32	304	13.2	33	2.5	140	1.85
H	35	376	10.6	25	0.8	310	1.65
I	23	230	5.7	36	0.9	200	1.60
J	30	288	5.0	19	2.0	430	1.90
Mean	27.6	280.5	6.95	30.6	1.6	298	2.09

The subscript max (or min) refers to the maximum (or minimum) values observed for the response parameters defined: p, peak amplitude of the poststimulus time histogram in impulses/6 ms bin/16 stimuli; f, median of the maximum instantaneous frequency in impulses per second; n, average number of impulses evoked per stimulus; Q_L, interquartile range of the first spike latency in milliseconds; a, amplitude of the proximal negative response in microvolts.
D is the dynamic range of the proximal negative response in log units of intensity.

range (the intensity range over which the response amplitude changes from 10 to 90% of its maximum value) for B (2.1 log units) is equal to the mean for all 11 preparations (see Table I) and is also quite similar to that obtained with single well spaced flashes in frog (Burkhardt, 1970) and *Necturus* (Proenza and Burkhardt, in preparation). It is a noteworthy feature of Fig. 4 that the close relation between the PNR and PSTH holds well in spite of differences in dynamic range (E vs. C) and absolute sensitivity of the neurons under test (J vs. B, Fig. 2). This strongly suggests that the PNR is very closely linked to mechanisms which trigger the excitation of on-off neurons.

To examine the relation between the peak amplitudes of the PNR and PSTH more directly, we plot them against each other in Fig. 5. The straight lines represent the best-fitting linear regression equation: $P = bA + k$, where P is the normalized peak amplitude of the PSTH ($P = p/p_{max}$), A is the nor-

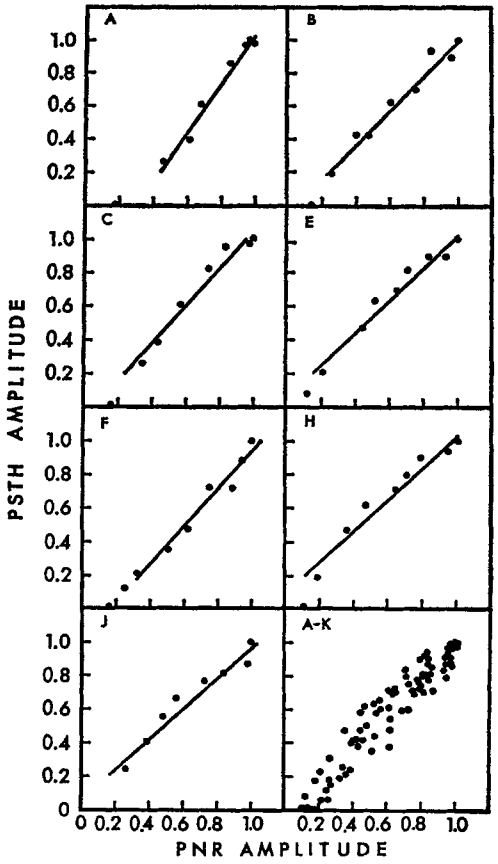

FIGURE 5. Relation between the peak amplitude of the PSTH of single on-off neurons and the peak amplitude of the PNR. Lower right panel (A-K) shows data pooled from 11 preparations. Results for seven of these are shown in the other panels along with with the best-fit line. See text for details.

malized peak amplitude of the PNR ($A = a/a_{max}$), b is the slope and k, the y-intercept. The straight lines approximate the data reasonably well over the range shown, which excludes the intensity region where the neuron fails to respond to every flash. As an index of goodness of fit, the standard error of estimate for predicting the normalized peak amplitude of the PSTH from the normalized peak amplitude of the PNR was calculated. These and the slope values are in Table II. Thus, 9 of the 11 preparations yield slope values near 1.0 (± 0.12) and the standard errors range from 0.04 to 0.07. The seven preparations of Fig. 5 include the cases with the lowest (J) and highest (A) slopes and the smallest (A) and largest (C) standard errors. Results from all 11 preparations are pooled in the lower right of Fig. 5. If the entire PSTH response range is considered, both these pooled results and most individual plots can be fit somewhat better by an equation yielding curves of slight negative acceleration than by the linear equation used above. But there seems little utility or insight to be gained from this tactic at present. Thus, we simply conclude that the peak amplitude of the suprathreshold PSTH of single on-off neurons is approximately linearly related to the peak amplitude of the PNR simultaneously recorded.

Having found a rather simple and general relation between the PNR and PSTH, we next consider two traditional measures of the impulse discharge: the average number of impulses evoked and the maximum instantaneous frequency. The maximum average number of impulses evoked, n_{max}, is listed in Table I for each preparation. For further analysis, we use the normalized response measure, $N = n/n_{max}$, and will refer to this as the relative number of impulses. In some cases, the relation between the relative number of impulses and stimulus intensity was very similar to that found between the nor-

TABLE II

SUMMARY OF PNR AMPLITUDE-NEURON RESPONSE BEST-FIT ANALYSIS

Preparation	Slope			Standard error of estimate		
	P	*F*	*N*	*P*	*F*	*N*
A	1.48	0.92	1.16	0.04	0.06	0.04
B	1.03	1.06	1.15	0.05	0.05	0.05
C	1.12	0.87	0.67	0.07	0.04	0.06
D	0.90	0.68	0.85	0.04	0.03	0.04
E	0.95	0.21	0.68	0.05	0.02	0.09
F	1.12	0.22	0.86	0.05	0.03	0.03
G	1.12	0.94	1.05	0.05	0.04	0.09
H	0.93	0.53	0.83	0.06	0.02	0.07
I	0.90	0.88	0.57	0.07	0.07	0.12
J	0.89	0.67	0.71	0.05	0.06	0.03
K	1.24	1.24	0.81	0.04	0.06	0.09
Mean	1.06	0.75	0.85	0.05	0.05	0.07

malized peak amplitude of the PSTH and intensity. So the plot of either measure against normalized PNR peak amplitude yielded almost identical slopes for the best-fit calculation. But in general, the slope found for the relative number of impulses was less than that found for PSTH peak amplitude. The former measure also gave some large standard errors (see column *N* in Table II). Thus, the relative number of impulses evoked may be approximately linearly related to the peak amplitude of the PNR but the relation is different in slope and sometimes considerably less precise than that found between the peak amplitudes of the PSTH and PNR. We will not further consider the relative number of impulses evoked, for this measure seems unlikely to be of direct functional significance for intensity coding: even if a neural mechanism is conceived to effectively count spikes, a decision about intensity would often hinge critically upon the last impulse in the spike train.

To evaluate the relation between the maximum instantaneous frequency of the discharge and the PNR, we measured the minimum interspike interval for each discharge evoked, computed the median for each intensity level, and converted these values to frequency, f, in impulses per second. The maximum value obtained in each preparation, f_{max}, is listed in Table I. For further analysis, we will use the normalized measure, $F = f/f_{max}$, and refer to this as the relative peak frequency. Plots of this measure against the corresponding peak amplitude of the PNR were found to be approximately linear as shown in Fig. 6 which includes the preparations giving the minimum and maximum best-fit slopes. Slope and standard error values of the best-fit calculations for all preparations are listed in column *F* of Table II.

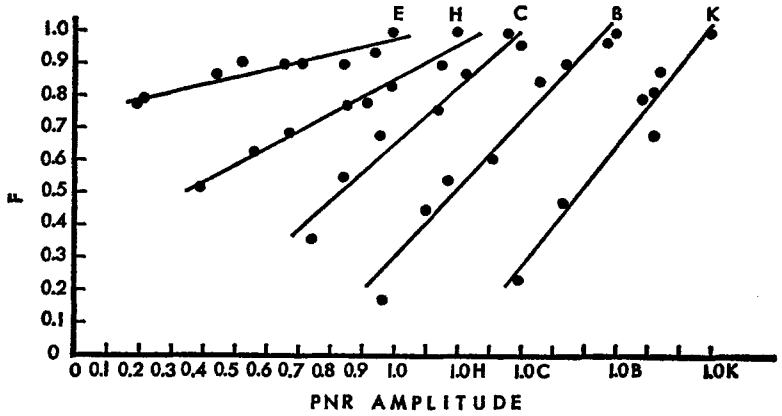

FIGURE 6. Relation between relative peak frequency, *F*, of five on-off neurons and the peak amplitude of the simultaneously recorded PNR. Data for all preparations except *E* are shifted to the right as indicated by the location of the 1.0 points on the abscissa. See text for further definition of *F* and other details.

The agreement between the intensity-response curves based on relative peak frequency (F) and peak amplitude of the PSTH was found to vary from one neuron to the next. This result is indicated by the slope values found in columns P and F of Table II and is illustrated in Fig. 7 where intensity-response curves are shown for four neurons. The squares represent the relative peak frequency measure (F) and the solid circles, the normalized peak amplitude of the poststimulus time histogram (P). (We will discuss the open circles later). For neuron E, there is a surprisingly marked disparity in the behavior

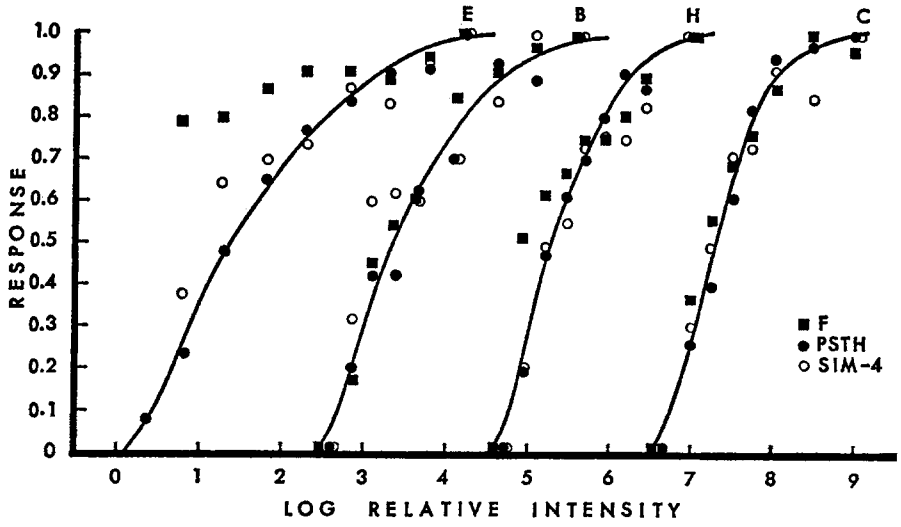

FIGURE 7. Intensity-response data for four on-off neurons for two response measures based on 16 responses per intensity level: relative peak frequency (squares) and PSTH peak amplitude (closed circles). Open circles refer to simulation results based on four response samples. For details of simulation, see Discussion. Curves are drawn by eye and their lateral separation and position are arbitrary. See Fig. 2 for the neurons' absolute sensitivity.

of these two response measures. This finding can be better understood by considering the temporal variability of the spike discharge.

We examined the variability of the first spike latency and the variability of the minimum interspike interval, using an index appropriate for small samples: The interquartile range, Q. Thus, Q_L is the time range which includes the central half of the first spike latency distribution. Similarly, Q_I is the interquartile range of the minimum interspike interval distribution. These measures of temporal variability are plotted against stimulus intensity in Fig. 8 along with I_m, the median of the minimum interspike interval (i.e. the measure from which f was calculated, see above). For neuron B in Fig. 8, all three features of the discharge decrease in much the same way and so all evidently contribute to the initial growth of PSTH amplitude with intensity.

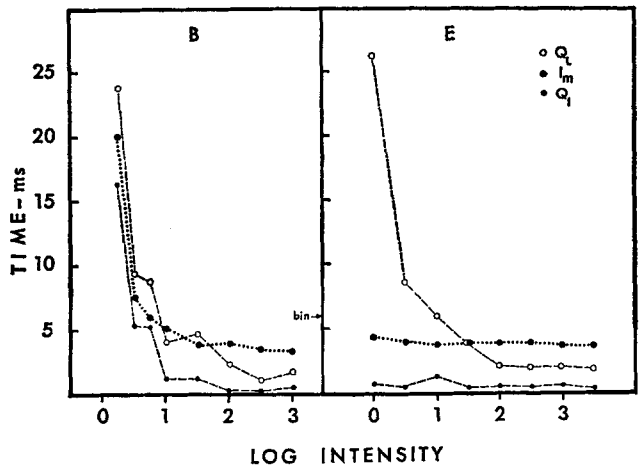

FIGURE 8. Relation between stimulus intensity and some temporal properties of the impulse discharge for two neurons (*B* and *E*). Q_L (open cirlces) is the interquartile range of the first spike latency. Q_I (small filled circles) is the interquartile range of the minimum interspike interval, and the median of the latter (I_m) is shown by large filled circles. See text for further definition of response measures. The arrow on the middle ordinate is at 6 ms, the bin width used in PSTH analyses. The intensity scale is arbitrary. See *B* and *E* in Fig. 2 for absolute sensitivity.

But the situation is considerably different for neuron *E*. At the lowest intensity, the large value of Q_L shows that there is considerable temporal jitter in the latency of the first spike from flash to flash. In contrast, the minimum interspike interval and its variability are quite small. And as intensity is increased, only the variability of latency decreases appreciably. It is thus evidently a primary factor responsible for the growth of PSTH amplitude with intensity (see *E* in Fig. 7). In general, the variability of the first spike latency decreased by a factor of 20–30 over the intensity range, as may be seen in Table I where the maximum and minimum values of Q_L are listed for each neuron. Since the first spike latency was also always found to systematically decrease with intensity (see Fig. 1), our findings may be put in clearer perspective: As the latency of the first spike decreases with intensity so does its absolute variability. From the analysis of Fig. 8 and the latency variability data of Table I, we conclude that temporal jitter of the first spike latency must be an important factor influencing PSTH amplitude. If the PSTH is a functionally relevant index (see Discussion), these results then suggest that temporal jitter of latency is an important factor in intensity coding.

At low intensities, the variability of the minimum interspike interval will also have some influence on PSTH amplitude. Of the neurons studied, *B* and *E* represent extremes. For the majority, the variability of the minimum interspike interval (Q_I) showed some tendency to decrease with intensity.

But even at the lowest intensity, it was typically 3 ms or less (half the value of the bin width used for the PSTH). Thus, of the two types of temporal variability considered, that of the first spike latency seems to exert the greater influence on PSTH peak amplitude. In sum, although the measures of Fig. 8 cannot fully characterize the PSTH, they usefully distinguish several individual factors which contribute to it. By thereby underscoring the influence of temporal variability, we conclude, at least for the neurons of this study, that the PSTH peak amplitude and the peak frequency of the impulse discharge should be approached as intrinsically different measures of excitability even though both can be and often are scaled in the same unit (spikes per second).

DISCUSSION

Retinal Impulse Activity and Intensity Coding

In his recent monograph, Brindley (1970) suggests that the intensity-response relations of retinal ganglion cells are rarely simple or regular (see also Lipetz, 1969) and we know of no adequate studies using single response measures whose results clearly contest this view. In some contrast, we show here that the PSTH of frog on-off neurons gives rather simple and uniform intensity-response relations and recent PSTH studies of cat ganglion cells also show some orderly stimulus-response curves (Cleland and Enroth-Cugell, 1970; Creutzfeldt et al., 1970; Ogawa et al., 1966; Stone and Fabian, 1968; Winters and Walters, 1970). However, behaviorally relevant coding of light intensity must be based on a single stimulus, not 16. Can the PSTH be translated into terms pertinent to intensity coding of single stimuli?

Others have previously sketched the idea that the experimental operations used to extract the PSTH could be analogous to a spatiotemporal averaging process which the nervous system performs for a single stimulus (Perkel and Bullock, 1972; Maffei, 1968). To pursue this idea explicitly, we propose a specific mechanism with the following features: (*a*) A single small stimulus efficiently activates several afferent channels (ganglion cells). (*b*) The fine temporal structure of the evoked impulse activity varies across channels, much as does a single neuron's response to a series of identical stimuli. (*c*) These afferent channels converge upon a more proximal neuron. The amplitude of the resulting postsynaptic potential is the signal for light intensity. It is formed by the temporal summation of the unit synaptic potentials triggered by the impulses of the afferent barrage.

To evaluate this proposal more directly, we simulated the mechanism. The actual impulse discharge of a neuron was fed to an R-C network which produced an output representing the temporal summation of all unit "synaptic" potentials evoked. The time-course of the unit synaptic potential was

selected to closely duplicate that found in the frog nervous system (McClennan, 1963; also see below). To simulate different numbers of afferent channels, we varied the number of responses sampled, using the computer to continue the summation process. Responses simulated in this way for neuron *H* are shown in Fig. 9 as a function of stimulus intensity for sample sizes of 4 and 8. In total, we examined the simulated responses of four neurons using three sample sizes (4, 8, 16) and three decay time constants of the unit potential (6, 12, and 18 ms with a constant rise time of 1 ms —see 12 ms example, U, in Fig. 9). The resulting amplitude-intensity curves were in all cases similar to the neuron's PSTH curve. Although increasing the sample size in-

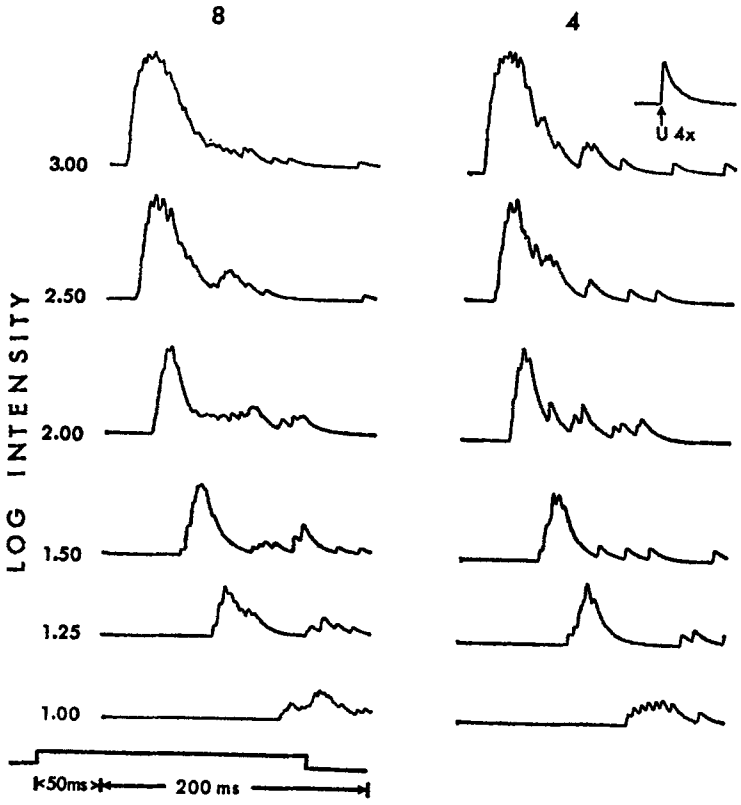

FIGURE 9. Responses simulated from the impulse discharge of neuron *H* as fully described in the text. Left and right columns are based on eight and four response samples, respectively; the intensity level for horizontally aligned responses is indicated at the far left. For both columns, the records start 50 ms after stimulus onset as indicated by the stimulus marker at left below. The display gain for the left column is half that of the right to approximately equate the maximum responses. The inset at the upper right, U 4x, shows the waveform of the unit "synaptic" potential used; it is displayed at a gain 4 times that used for the main responses of the right column. See text for discussion and details.

creased the similarity as expected, a sample size of only 4 was found to give a rather orderly stimulus-response curve. The latter point is illustrated in Fig. 7 where the open circles are simulation results for a sample size of 4.

These simulation results thus suggest that the proposed mechanism, when using a modest number of channels (4–8), will generate orderly stimulus-response curves and mimic the behavior of the PSTH. This outcome reinforces the idea that the PSTH may reflect a functionally significant process for intensity coding. If so, several parameters of the neuronal discharge of the retina now assume importance for intensity coding. One of these, temporal jitter of latency (Q_L), has received scant attention previously, but the absence of spontaneous activity in the neurons studied here has allowed us to demonstrate its potent and relatively independent role in shaping the peak amplitude of the PSTH. Temporal jitter of latency may be similarly important for most sensory neurons: It is a very general finding that response latency decreases with the strength of the stimulus and it is to be expected that the absolute variability of latency (Q_L) will also concomitantly decrease. Our results (Fig. 8 E) also raise the interesting possibility that neurons which individually show but limited capacity for frequency modulation may nevertheless be capable of transmitting an intensity code in concert by means of changes in temporal jitter. Thus, *Necturus* amacrine cells, whose sparse impulse discharge appears not to be intensity dependent (Dowling and Werblin, 1971), might still en masse convey some intensity information to another amacrine cell or ganglion cell.

Whatever the limitations of the mechanism proposed, it is probably closer to the basis of intensity coding than the simplistic single-channel single-parameter mechanisms commonly offered. The modest number of channels needed is realistic, given the large overlapping receptive fields (Barlow, 1953 *b*), high ganglion cell density (Maturana et al., 1960), and evidence for central convergence in the frog visual system (Lettvin et al., 1961). In the cat, there is also evidence for imperfect temporal correlation between the maintained and spontaneous activity of neighboring ganglion cells (Rodieck, 1967; Gestri et al., 1966).

Relations between Retinal Impulse Activity and the PNR

Previous work has shown that the frog PNR is highly correlated with the threshold excitability of single on-off neurons (Burkhardt, 1970; Burkhardt and Berntson, 1972). The findings reported here now extend the correlation to the suprathreshold domain. To our knowledge, this is the first report to reveal a relatively simple quantitative relation between parameters of the impulse discharge of single neurons and the magnitude of a graded potential in the vertebrate retina. Thus, quite apart from the comments advanced below, the evidence accumulated to date strongly suggests that the PNR is

intimately allied with the mechanisms responsible for transmission of visual information over local pathways in the proximal retina.

Several converging arguments suggest that the PNR mainly reflects the graded activity of amacrine cells (Burkhardt, 1970) and we will now accept this as a working hypothesis. There is anatomical and physiological evidence that amacrine cells provide the main synaptic input to amphibian on-off ganglion cells (Dowling, 1968; Werblin and Dowling, 1969). Thus, if at least some of the neurons studied here are representative of on-off ganglion cells as seems highly probable (see Methods), the present results have implications for amacrine-ganglion cell coupling. They suggest that the overall transfer from the graded activity of amacrine cells to the impulse output of on-off ganglion cells is relatively simple: The ganglion cell's suprathreshold discharge, specified as PSTH peak amplitude or as maximum frequency, is approximately a linear function of the peak amplitude of the graded activity of a local population of amacrine cells. The simplest extension of this view suggests that the synaptic transmission from amacrine to ganglion cell is a nearly linear process. Thus, the sequence of events: graded amacrine potential—graded ganglion cell potential—impulse discharge, might simply involve two nearly linear transforms.

This research was supported by a grant (EY-00406) from the National Eye Institute, U. S. Public Health Service and by a grant from the Graduate School of the University of Minnesota.

Dr. Whittle was on leave from The Psychological Laboratory, University of Cambridge, Cambridge, England, and has now returned there.

Received for publication 25 September 1972.

REFERENCES

BARLOW, H. B. 1953 *a*. Action potentials from the frog's retina. *J. Physiol.* (*Lond.*). **119**:58.

BARLOW, H. B. 1953 *b*. Summation and inhibition in the frog's retina. *J. Physiol.* (*Lond.*). **119**:69.

BRINDLEY, G. S. 1970. Physiology of the Retina and Visual Pathway. The Williams & Wilkins Company, Baltimore. 82.

BURKHARDT, D. A. 1970. Proximal negative response of frog retina. *J. Neurophysiol.* **33**:405.

BURKHARDT, D. A., and G. G. BERNTSON. 1972. Light adaptation and excitation: lateral spread of signals within the frog retina. *Vision Res.* **12**:1095.

CLELAND, B. G., and C. ENROTH-CUGELL. 1970. Quantitative aspects of gain and latency in the cat retina. *J. Physiol.* (*Lond.*). **206**:73.

CREUTZFELDT, O. D., B. SAKMAN, H. SCHEICH, and A. KORN. 1970. Sensitivity distribution and spatial summation within receptive-field center of retinal on-center ganglion cells and transfer function of the retina. *J. Neurophysiol.* **33**:654.

DOWLING, J. E. 1968. Synaptic organization of the frog retina: an electron-microscopic analysis comparing the retinas of frogs and primates. *Proc. R. Soc. Lond. B. Biol. Sci.* **170**:205.

DOWLING, J. E., and F. S. WERBLIN. 1971. Synaptic organization of the vertebrate retina. *Vision Res.* (Suppl. 3):1.

FATECHAND, R. 1971. The a_2 component of the vitreal a-wave and its intraretinal localization in the frog retina. *Vision Res.* **11**:489.

FOX, S. S., and J. H. O'BRIEN. 1965. Duplication of evoked potential wave-form by curve of probability of firing of single cell. *Science* (*Wash. D. C.*). **147**:888.

GESTRI, G., L. MAFFEI, and D. PETRACCHI. 1966. Spatial and temporal organization in retinal units. *Kybernetik.* **4**:196.

GRANIT, R. 1963. Sensory Mechanisms of the Retina. Hafner Publishing Co., Inc., New York.

GRÜSSER-CORNEHLS, U., O. J. GRÜSSER, and T. BULLOCK. 1963. Unit responses in the frog's tectum to moving and nonmoving visual stimuli. *Science* (*Wash. D. C.*). **141**:820.

HARTLINE, H. K. 1938. The response of single optic nerve fibers of the vertebrate eye to illumination of the retina. *Am. J. Physiol.* **121**:400.

HARTLINE, H. K. 1940 *a*. The receptive fields of optic nerve fibers. *Am. J. Physiol.* **130**:690.

HARTLINE, H. K. 1940 *b*. The effects of spatial summation in the retina on the excitation of the fibers of the optic nerve. *Am. J. Physiol.* **130**:700.

HOLDEN, A. L. 1972. Proximal negative response in the pigeon retina. *J. Physiol.* (*Lond.*). **221**:173.

KANEKO, A. 1970. Physiological and morphological identification of horizontal, bipolar and amacrine cells in the goldfish retina. *J. Physiol.* (*Lond.*). **207**:623.

LETTVIN, J. Y., H. R. MATURANA, W. H. PITTS, and W. S. MCCULLOCH. 1961. Two remarks on the visual system of the frog. *In* Sensory Communication. W. A. Rosenblith, editor. John Wiley & Sons, Inc., New York. 773.

LIPETZ, L. E. 1969. The transfer functions of sensory intensity in the nervous system. *Vision Res.* **10**:1205.

MAFFEI, L. 1968. Spatial and temporal averages in retinal channels. *J. Neurophysiol.* **31**:283.

MATSUMOTO, N., and K.-I. Naka. 1972. Identification of intracellular responses in the frog retina. *Brain Res.* **42**:59.

MATURANA, H. R., J. Y. LETTVIN, W. A. MCCULLOCH, and W. H. PITTS. 1960. Anatomy and physiology of vision in the frog (*Rana pipiens*). *J. Gen. Physiol.* **43**(Part 2):129.

MCLENNAN, H. 1963. Synaptic Transmission. W. B. Saunders Company, Philadelphia. 33.

OGAWA, T., P. O. BISHOP, and W. R. LEVICK. 1966. Temporal characteristics of responses to photic stimulation by single ganglion cells in the unopened eye of the cat. *J. Neurophysiol.* **29**:1.

PERKEL, D. H., and T. H. BULLOCK. 1972. A table of candidate neural codes or forms of representation of information in the nervous system. *In* Sensory Coding. W. R. Uttal, editor. Little, Brown and Company, Boston. 97.

REUTER, T. 1969. Visual pigments and ganglion cell activity in the retinae of tadpoles and adult frogs (*Rana temporaria* L.). *Acta Zool. Fenn.* **122**(Separatum):64 pp.

RODIECK, R. W. 1967. Maintained activity of cat retinal ganglion cells. *J. Neurophysiol.* **30**:1043.

STONE, J., and M. FABIAN. 1968. Summing properties of the cat's retinal ganglion cell. *Vision Res.* **8**:1023.

TOMITA, T., and Y. TORIHAMA. 1956. Further study on intraretinal action potentials and on the site of ERG generation. *Jap. J. Physiol.* **6**:118.

WERBLIN, F. S., and J. E. DOWLING. 1969. Organization of the retina of the mudpuppy, *Necturus maculosus*. II. Intracellular recording. *J. Neurophysiol.* **32**:339.

WINTERS, R. W., and J. W. WALTERS. 1970. Transient and steady state stimulus-response relations for cat retinal ganglion cells. *Vision Res.* **10**:461.